

A Methodology for Determination of Approximate Technically Recoverable Hydrokinetic Potential for Hydrokinetic Farming in River or Canal

Umanshankar Sharma, D. K. P. Singh, Senior Member IEEE, D. K. Khatod Senior Member IEEE

Abstract

The need of electrical energy is everlasting and with the rapid depletion of non renewable energy sources, different renewable energy sources are explored. Amongst the renewable energy sources the hydrokinetic turbines is identified to be very promising because theoretically calculated hydrokinetic potential seems to very large at many locations. The recoverable hydrokinetic potential obtained by data collected from actual locations differs due to various reasons. Presence of hydrokinetic turbine in river or canal creates wake up effects and back effects reducing the water velocity. In this paper, this dragging effect of turbines present in water is incorporated into effective Manning's coefficient by hydrologic computations. Simulation of water flow in river or canal segment is performed with available discharge data from flow duration curve in Hydrological Engineering Centre-River Analysis System with geometric parameters of river segment from Google Earth. The approximate technically recoverable hydrokinetic potential, optimized size, number of hydrokinetic turbines, and placement of turbines in hydrokinetic farming at identified river segment are presented. The proposed method saves the time and cost incurred in data collection from location which in turn helps in efficient planning.

I Introduction

Renewable energies give a good context to be an option to fossil and nuclear fueled power plants to meet everlasting demand of electrical energy. Energy from water can be harnessed in two ways one the conventional hydropower plants utilizing hydrostatic energy by impoundment of water behind dams for creating a hydraulic head for generating electricity [1] and other hydrokinetic energy conversion where kinetic energy of flowing water is used for generation of electricity [2]. Stream hydrokinetic energy is captured from natural flow of water in rivers, manmade canals etc. The amount of electricity that can be generated from hydrokinetic energy source is reliant on the volume and velocity of the flowing water resource. Amongst the various concepts of conversion of hydrokinetic energy into electrical energy, the turbine system has been the most common and proven but the velocity of flowing water should be 0.5 m/s or more for successful operation of extraction of electrical energy [3]. The technology of hydrokinetic is gaining popularity as one of the renewable energy source needing further investigations. Similar to wind energy conversion system, the total available active power captured by hydrokinetic turbine is reliant on the density, cube of velocity, cross sectional area and power coefficient as enumerated in equ (1).

$$P_a = \frac{1}{2} A \rho V^3 C_p \quad (1)$$

Here 'A' is the turbine area in m², 'ρ' the water density (1000kg/m³), 'V' the stream water velocity (m/s) and 'C_p' the power coefficient or efficiency of hydrokinetic turbine which is 16/27=0.592 (theoretical portion of power available).

The power coefficient 'C_p' implies that the hydrokinetic turbine can generate a portion of the total kinetic power. This coefficient is limited to 16/27=0.592 by Betz law [4]

$$C_p = \frac{1}{2} \left(1 + \frac{v_o}{v_i}\right) \left(1 + \frac{v_o^2}{v_i^2}\right) \quad (2)$$

Hydrokinetic calculator [5] for assessment of hydrokinetic potential in rivers was based on two dimensional hydrodynamic numerical models developed at the National Center for Computational Hydro Science & Engineering, University of Mississippi resulting in the velocity outputs. These results obtained are used to compute the instantaneous power density, an essential element in calculating the hydrokinetic power of a river reach. The computational domain, maximum velocity and specific discharge were identified for each river cross section in estimating the stability of the river reach and thus, the feasibility of installing hydrokinetic turbine. The capacity of coupling measurements of river velocity derived from Moderate Resolution

Imaging Spectroradiometer (MODIS) and water levels derived from ENVISAT Advanced Radar Altimeter (RA-2) for river discharge estimation is thoroughly investigated. The coupling of the two sensors provides good accuracy of hydraulic quantities for discharge estimation. The sensors are utilized for assessment of hydraulic quantities [6] & [7] which may suffer the sensitivity issues over a period of time and the location of sensors is another important aspect affecting the estimation of potential of hydrokinetic energy largely. Rather than collecting the data from different locations, the estimation of hydrokinetic potential from remote locations is preferable for identified site /s resulting in saving of time and cost incurred. The proposed method gives a good estimate of the hydrokinetic potential at gauged site from remote locations saving the time and cost helping efficient planning.

II Proposed Methodology

For the river or canal segment under study the data like monthly/ weekly discharge, plot of flow duration curve, Digital Elevation Model, Bathymetric data if possible, and channel roughness (Manning's coefficient) are explored.

The river line hydrokinetic active power (P_{th}) theoretically available in a given river /canal segment can be defined as

$$P_{th} = \gamma Q \Delta H \quad (3)$$

Here ' γ ' is specific weight of water ($9.81 \times 10^3 \text{ Nm}^3$), ' Q ' is discharge (m^3/s); $\Delta H (= BS.L)$ is level difference in entry and end of water surface level in river segment (m), ' BS ' is average bed slope and ' L ' is length of segment (m).

The river line hydrokinetic active power (P_{tech}) for selected river segment is the recoverable fraction of the theoretically calculated power under the technical constraints and assumptions [3] River Analysis System (HEC-RAS) software from Hydrologic Engineering Center's (CIEWR-HEC) provides tools for user to simulate one-dimensional steady flow, one and two-dimensional unsteady flow for river or channel [8]. Simulation in HEC RAS is done utilizing the channel geometry, Manning's coefficient (separately for left bank, right bank and main channel), slope and various condition obtained from flow duration curve. From simulation results the depth of water and average velocity are recorded. If the water depth is below 2 m or average water velocity is less than 0.5 m/s than deployment of hydrokinetic farming in given segment is not technically feasible hence, other site is explored for study.

Let ' D_{90} ' be the water depth at 90 percentage flow when no hydrokinetic devices are present. Diameter of turbine (D) can be selected of size 80 percentage of ' D_{90} '. The presence of the hydrokinetic turbines would result wake up effects and back effects resulting in decrease of water velocity and increase in water depth. This dragging effect in presence of these devices can be incorporated in to effective Manning's coefficient ' n_e ' from natural channel bottom Manning's coefficient ' n ' [9].

$$n_e = n (b^{1/3} - 0.28263.b^{-1/3} - 0.139296)^{5/3} \quad (4)$$

$$\text{Where } b = 0.46088a + ((0.46088.a + 0.68368)^2 + 0.022578)^{1/2} + 0.68368 \quad (5)$$

$$\text{Here } a = \left(\frac{3\xi(1+\epsilon)NA_r}{4n^2g.wL} \right)^{3/2} \cdot \sqrt[3]{h} \quad (6)$$

Where ' ξ ' is turbine efficiency, ' ϵ ' blockage ratio (fraction of river cross-section occupied by devices), ' N ' is total number of devices in river segment, ' A_r ' is the frontal (or swept) area of the device (m^2), ' h ' is water depth (m), and ' w ' is the width of the river or channel that is occupied by device (m).

The Manning's coefficient is modified from ' n ' to ' n_e ' in HEC-RAS, and through simulation average velocity (V_{90}) and water depth which would result after placement of hydrokinetic devices are obtained. Total technical hydrokinetic potential ($P_{tech-90}$) in watts that can be recovered from the channel segment under consideration at 90 percentage flow will be

$$P_{tech-90} = \tau \frac{L}{2} (V_{90})^3 N . A_r \quad (7)$$

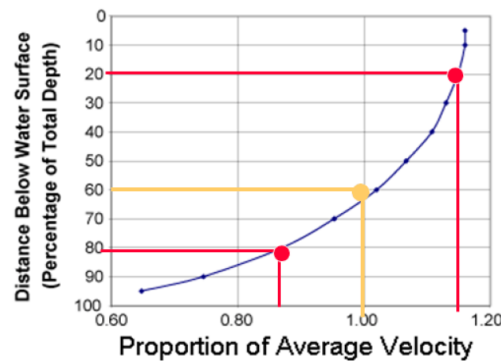


Fig. (1): Variation of Average Velocity with Depth

Water depth 'h' is obtained without placement of hydrokinetic devices through simulation in HEC-RAS for flow conditions of 90, 75, 50, 25, 5 (percentage of time). Using this obtained water depth modified Manning's coefficient is calculated using equ (4). Average velocities of water after placement of hydrokinetic turbines with new values of Manning's coefficient are obtained by simulating again. The velocity of water along the depth will vary as the portion of average velocity as shown in Fig. (1). The net velocity experienced by hydrokinetic turbine will be the velocity difference at height of ' $0.2 \times D_{90}$ ' from bottom of the channel to the velocity at height ' D_{90} ' from the bottom. These bottom and top water velocities experienced by hydrokinetic turbine can be found from the curve shown in Fig. (1) for river segment at Ramjhula for Ganga River selected for the study. Finally, the average velocity available for hydrokinetic turbine can be determined from weightage average of velocities obtained. Flow duration curve for the river segment under study is depicted in Fig. (2).

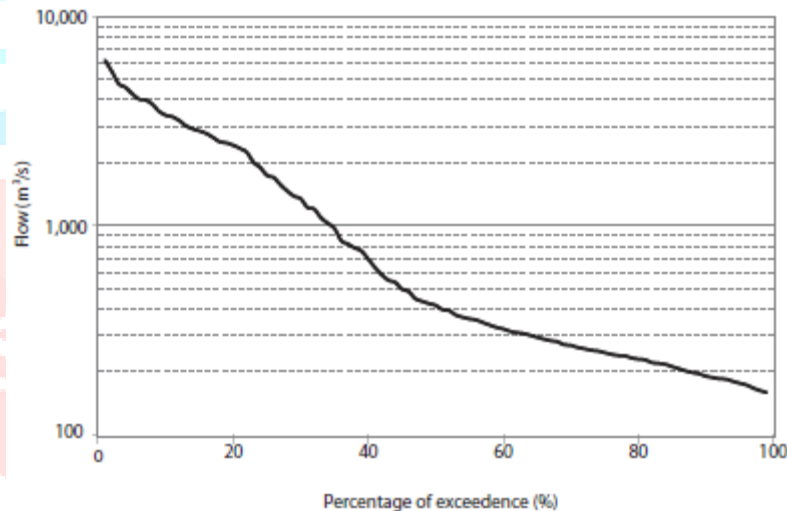


Fig. (2): Flow Duration Curve for River Segment at Ramjhula for Ganga River

River centre line, bank line, flow path line was drawn in Google Earth as depicted in Fig. (3). KML file was converted into raster layer in ARC MAP. SRTM Digital Elevation Model for the given site was downloaded from the site <https://earthexplore.usgs.gov/>. DEM obtained is referenced in HEC GEORAS for layer formation incorporating the surveyed data or real bathymetric data if available. The layers river, bank line, flow path line were formed by tracing the line converted from KML and the cross-section layer was formed as shown in Fig. (4). These layers are exported in GIS format. In HEC RAS, for river geometry, the layers that exported from HEC GEORAS were imported for simulation of river segment.



Fig. (3): River Center Line, Bank Line and Flow Path in Google Earth Pro at Ramjhula for Ganga River

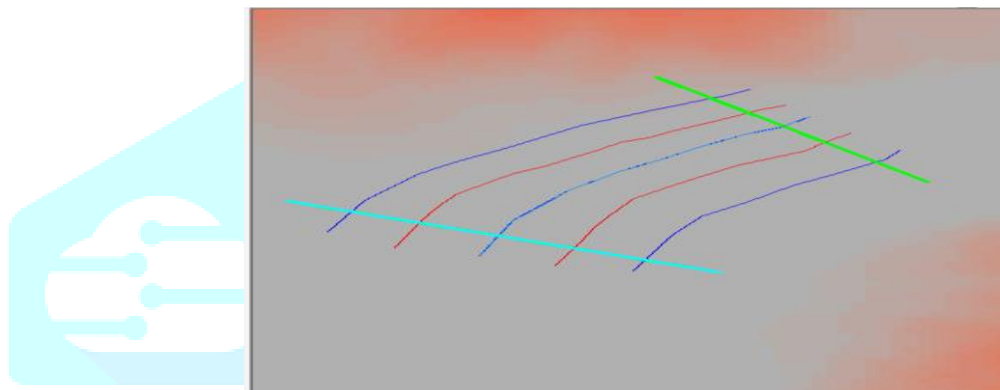


Fig. (4): Layer formation using HEC GEORAS, SRTM DEM and KML file (Google Earth) in Arc GIS

III Result

Simulation results in HEC RAS were obtained for 90%, 75%, 50%, 25% and 5 % flow discharge rates. The detailed results for 90% and 5% flow discharge rates are presented in this paper.

(a) At 90% flow discharge (200 m³/s)

The river segment under study was simulated in HEC RAS for 90 percent dependable flow. The water levels in the cross section of the river segment for upstream and downstream are shown in Fig. (5) & (6) respectively. The longitudinal water surface profile of the river, average velocity of water along the river segment and the top width of water along the river segment are shown in Fig. (7), (8), (9) respectively.

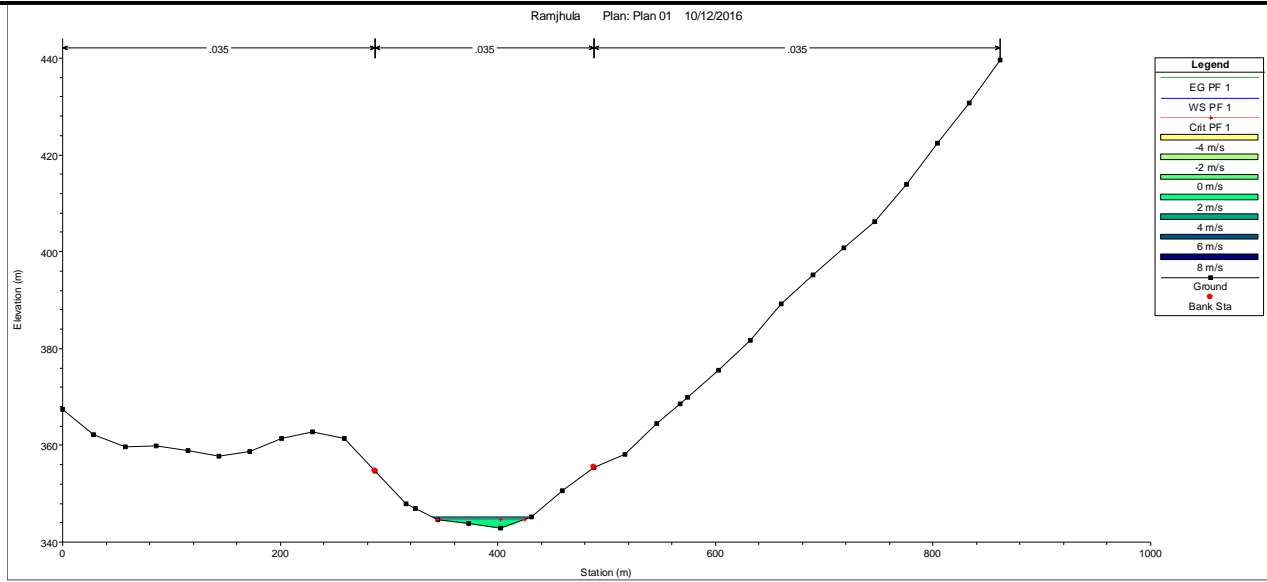


Fig. (5): Simulation Results for Upstream

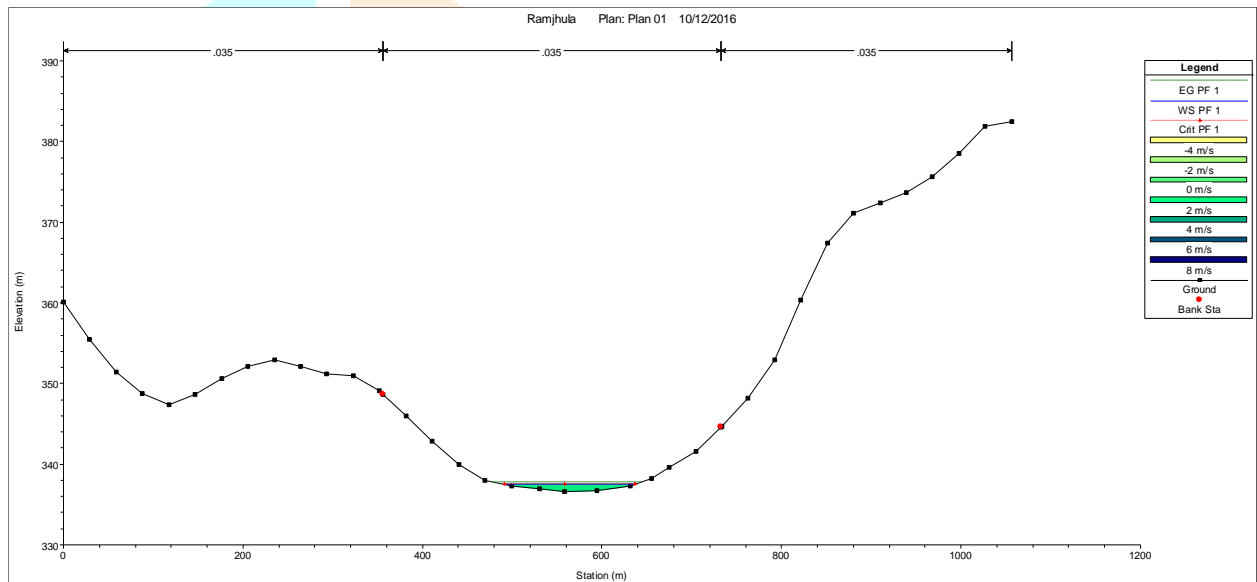


Fig. (6): Simulation results for downstream

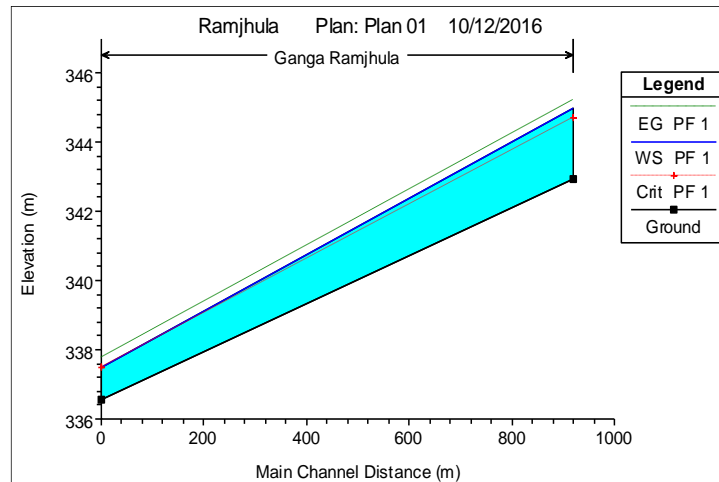


Fig. (7): Water surface profile

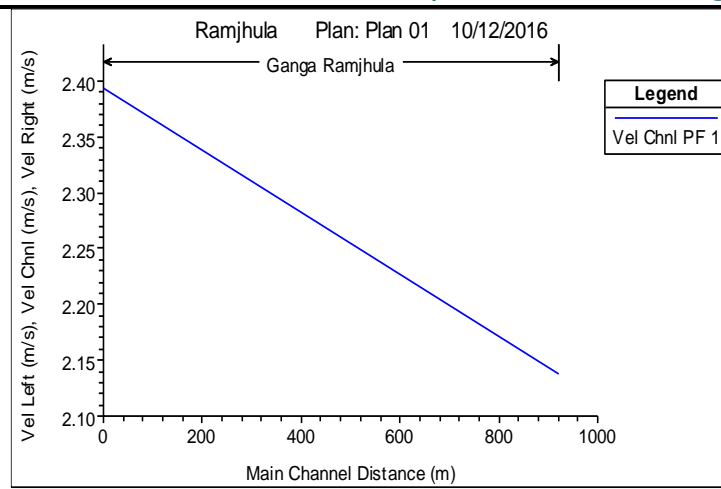


Fig. (8): Average Velocity Profile

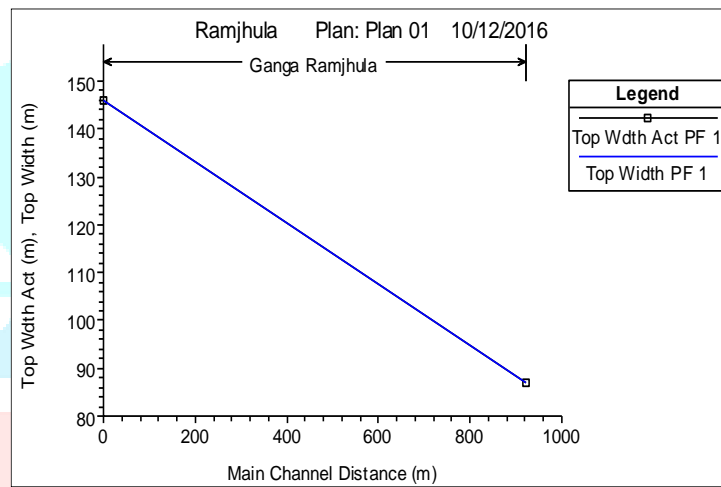


Fig. (9): Profile for Top Width of Water Surface

The water surface level difference between upstream and downstream can be calculated from Fig. (5) as,

$$\Delta H = 344.4 - 337.6 = 6.8 \text{ m}$$

We have $\gamma = 9800 \text{ Nm}^{-3}$ and $Q_{90} = 200 \text{ m}^3/\text{s}$

Theoretically, hydrokinetic potential at 90% dependable discharge = $\gamma Q \Delta H = 13328 \text{ KW}$

Now, technically recoverable hydrokinetic potential has to be calculated. Selecting diameter of turbine $D = 1.6 \text{ m}$ with 0.4 m for erection arrangement for bottom placement. Distance between rows = $10D = 16 \text{ m}$. Distance between columns = $2D = 3.2 \text{ m}$. Plot of cross sections at 16 m by interpolation in HEC RAS is depicted in Fig.(10).

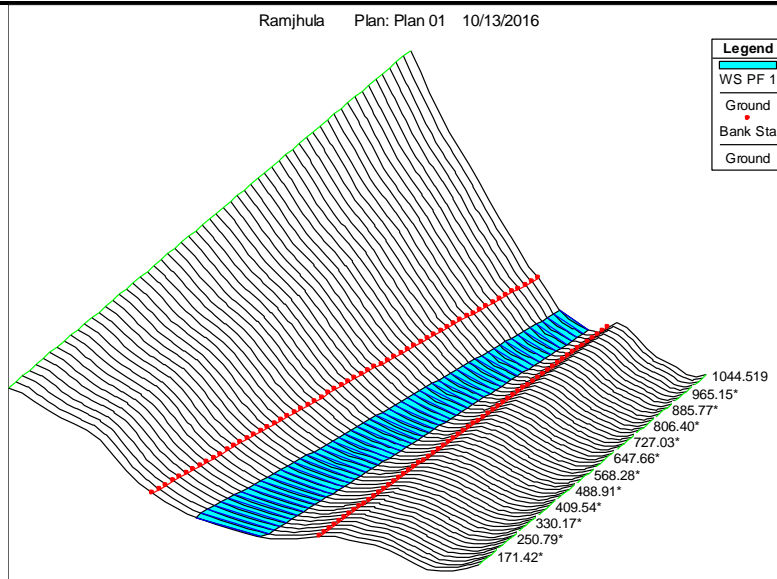


Fig. (10): Cross-sections by Interpolations

The number of turbines, blockage ratio etc are calculated utilizing the data obtained from Fig. (7 to 10) and is listed in Table (1).

Table (1): The Number of Turbines and corresponding Blockage Ratio

Sr. No.	XS position	Width for depth more than 2m	Top width	Flow Area	No of turbines	Turbine Area	Blockage Ratio
1	1044.51	20	83.63	80.61	6	12.06857143	0.149715562
2	1028.65	15	84.8	81.10	4	8.045714286	0.099207328
3	1012.77	14	85.96	81.55	4	8.045714286	0.098659893
4	996.90	12	87.15	82.02	3	6.034285714	0.073570906
5	981.02	10	88.34	82.48	3	6.034285714	0.073160593
6	965.15	10	89.53	82.96	3	6.034285714	0.072737292
7	949.27	10	90.73	83.38	3	6.034285714	0.072370901
8	933.40	8	91.92	83.78	2	4.022857143	0.048016915
9	917.52	6	93.11	84.12	2	4.022857143	0.047822838
10	901.65	6	94.08	84.45	2	4.022857143	0.047635964
11	885.77	4	94.86	84.78	1	2.011428571	0.023725272
12	869.90	Less than 2 m	95.7	85.07	N A		

After the cross section having the position at 869.90 m the depth of water was found less than 2 m along the cross section, hence, the hydrokinetic turbines could not be placed in that cross section of the river segment.

Average Blockage Ratio (ϵ) = 0.07, Manning’s Roughness coefficient (n) = 0.035

Turbine efficiency (ξ) = 0.35, Total number of devices in the given river segment (N) = 33

Frontal (or swept) area of the device (A_r) = 2.011 m², Water depth (h) = 2 m

Width of the river or channel that is occupied by devices (w) = 10.45m

Length of segment (L) = 159m, Overall efficiency = 0.3

Calculation for Effective Manning’s Roughness Coefficient (n_e):

$$a = \left(\frac{3}{4} \frac{\xi(1+\epsilon) N A_r}{n^2 g w L} \right)^{\frac{1}{3}} \sqrt[3]{h} = 1.1795$$

$$b = 0.46088a + ((0.46088.a + 0.68368)^2 + 0.022578)^{1/2} + 0.68368 = 2.4637$$

$$n_e = n (b^{1/3} - 0.28263.b^{-1/3} - 0.139296)^{5/3} = 0.0547$$

Effective Manning’s coefficient is increased because the dragging effect is created by placement of hydrokinetic turbines in water due to wake up effect and back effects. Simulating the flow condition in HEC RAS with effective Manning’s Roughness coefficient was performed. Simulated results for water surface and velocity are shown in Fig. (12) & (13) respectively.

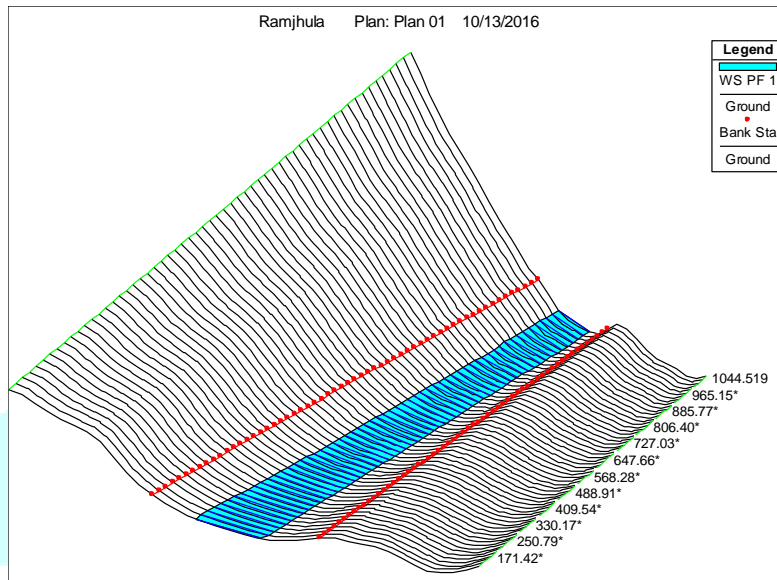


Fig. (11): Simulation Result for New Manning’s Coefficient

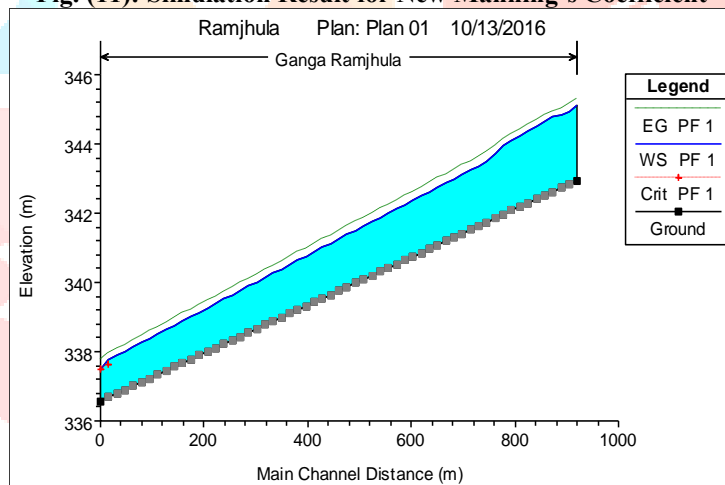


Fig. (12): Water Surface Plot

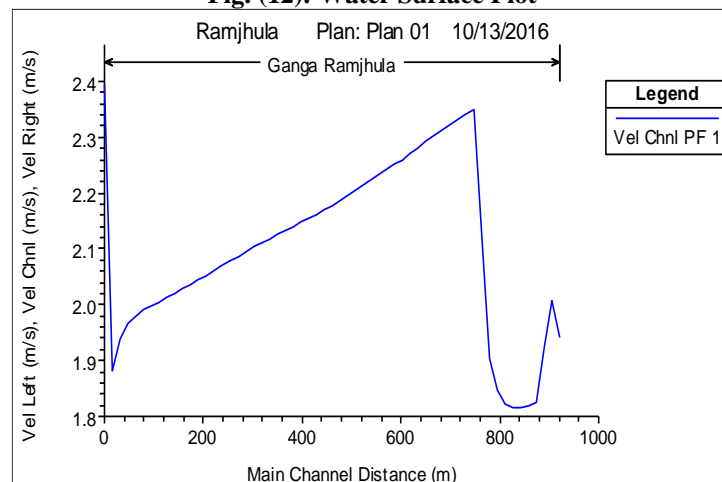


Fig. (13): Velocity Profile Plot

The recoverable hydrokinetic potential at 90% dependable flow for different turbine positions, number of turbines and velocity are listed in table (2).

Table (2): Technically Recoverable Hydrokinetic Potential

S.N.	XS position	No of turbines(N)	Velocity(V_{90}) m/s	$P_{tech-95} = \xi \frac{\rho}{2} (V_{90})^3 N A_r$ (in W)
1	1044.519	6	1.94	12219.12
2	1028.65	4	2.01	8017.46
3	1012.77	4	1.92	7890.20
4	996.90	3	1.82	5823.22
5	981.02	3	1.82	5823.22
6	965.15	3	1.81	5729.80
7	949.27	3	1.81	5729.80
8	933.40	2	1.82	3882.15
9	917.52	2	1.85	4008.73
10	901.65	2	1.91	4337.16
11	885.77	1	2.12	2956.27
Total Recoverable Hydrokinetic Potential at 90 % flow				66.417 KW

(b) At 5% flow discharge (600 m³/s)

Simulating HEC RAS without placement of turbine the water depth achieved 7 m. The water surface plot with and without placement of turbines and velocity profile are shown if Fig. (14), (15) & (16) respectively. Average blockage ratio is 0.07. The calculation of effective Manning's Roughness Coefficient (n_e) like in previous case yields the values of 'a', 'b', and ' n_e ' as 1.6806, 2.9242 and 0.0593 respectively.

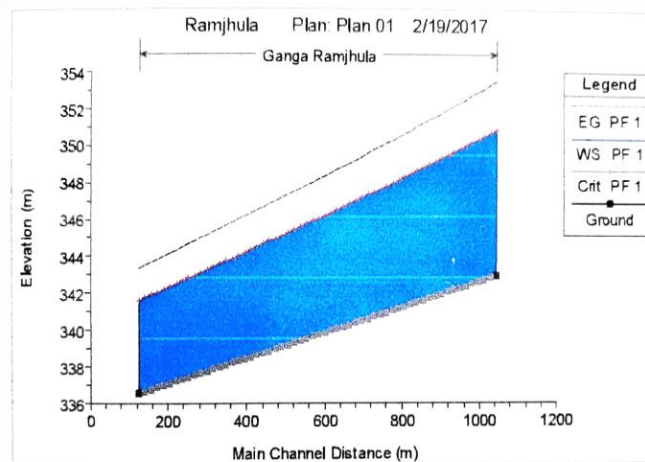


Fig. (14): Water Surface Plot for 5 % Flow without Placement of Turbines

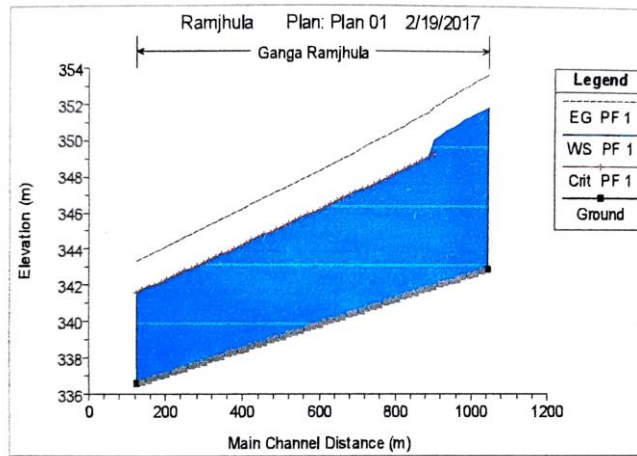


Fig.(15):. Water Surface Plot for 5 % Flow with Placement of Turbines

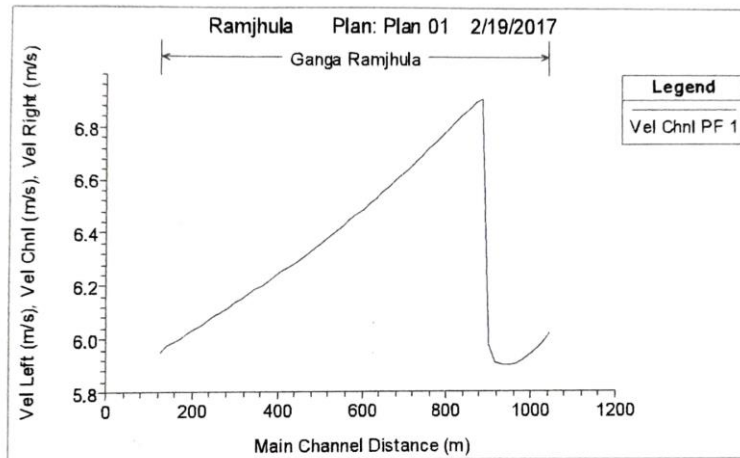


Fig. (16): Velocity Profile plot at 5% Flow with Placement of Turbines

The calculated blockage ratio with other details are depicted in Table (3) for 5 % flow discharge

Table (3): The Number of Turbines and corresponding Blockage Ratio

Sr. No.	XS position	Flow Area	No of turbines	Turbine Area	Blockage Ratio
1	1044.52	831.06	6	12.07	0.015
2	1028.65	834.63	4	8.05	0.010
3	1012.77	838.23	4	8.05	0.010
4	996.90	841.77	3	6.03	0.007
5	981.02	845.32	3	6.03	0.007
6	965.15	848.83	3	6.03	0.007
7	949.27	852.30	3	6.03	0.007
8	933.40	855.76	2	4.02	0.005
9	917.52	859.20	2	4.02	0.005
10	901.65	862.63	2	4.02	0.005
11	885.77	885.06	1	2.01	0.002

Interpolation between proportion of average velocity and total depth (d) from the curve shown in Fig. (1) was performed in MATLAB 2016a using polyfit function taking second order of polynomials.

$$V = -(0.8395).d^2 + 0.3154.d + 1.1338$$

Total recoverable hydrokinetic potential at 5 % flow is 1031.87 KW as depicted in table (4).

Table (4): Technically Recoverable hydrokinetic Potential at 5% flow

XS Position	Avg. Velocity	Ground Level	Water Sur. level	Depth pro.of turbine. (d)	Velocity pro. (V)	Velocity for turbine (Vs)	No of Turbines.	Potential(W)
1044.49	6.02	342.95	351.846	0.87	0.78	4.69	6	186207.56
1028.62	5.99	342.84	351.668	0.86	0.78	4.67	4	122845.48
1012.74	5.96	342.73	351.489	0.86	0.78	4.65	4	121577.23
996.87	5.94	342.62	351.306	0.86	0.78	4.65	3	90718.33
980.99	5.92	342.51	351.121	0.86	0.78	4.64	3	90274.57
965.12	5.91	342.4	350.932	0.86	0.78	4.64	3	90322.42
949.25	5.9	342.29	350.739	0.86	0.79	4.64	3	90401.31
933.37	5.9	342.18	350.539	0.86	0.79	4.65	2	60661.88
917.5	5.92	342.07	350.33	0.85	0.79	4.68	2	61732.12
901.62	5.97	341.96	350.082	0.85	0.79	4.73	2	63973.71
885.75	6.91	341.85	349.144	0.84	0.81	5.61	1	53149.04
Total Recoverable Hydrokinetic Potential at 5 % flow								1031.87 KW

The calculation steps for flow discharge of 90% and 5% are presented and for the 25%, 50%, 75% flow discharge rates the final recoverable hydrokinetic potential are listed in table (5). The power duration predicting the energy provided by the hydrokinetic plant at Ramjhula throughout the year for these flow discharge rates is shown in Fig. (17).

Table (5): Recoverable Hydrokinetic Potential

Sr. No.	Dependability	Discharge (m ³ /s)	Blockage Ratio	Water Depth(m)	Effective, Manning's Coefficient.	HKP Potential (kW)
1	25%	1800	0.017	4.4	0.0564	437.64
2	50%	400	0.047	2.43	0.0535	161.51
3	75%	250	0.06	2.02	0.0528	111.83

For the river segment under study the total number of hydrokinetic turbines are found to be 33 with radius of hydrokinetic turbines as 0.8m, the spacing between turbine row is 3.3 m with spacing between row is 16 m for hydrokinetic farming.

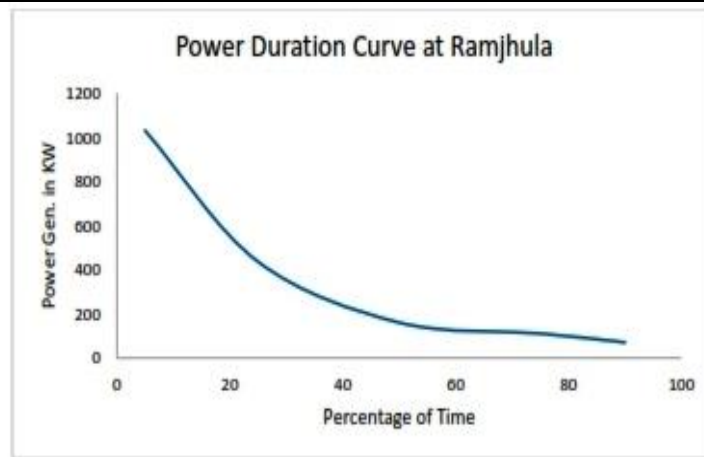


Fig. (17): Power Duration Curve at Ramjhula
IV Conclusions

A methodology for approximate technically recoverable hydrokinetic potential for river segment has been presented using DEM, HEC RAS and other hydrological computations. The technically recoverable hydrokinetic potential is found to be very less than theoretically calculated hydrokinetic potential incorporating the dragging effect created by waking up and back effects. The size, total number of turbines placements of turbines and the power duration curve throughout a year is obtained using the proposed method. In order to increase the accuracy of results rather than SRTM GLOBAL DEM of 1 arc second (30 m resolution) used in present case LIDAR DEM (2-3 , resolution) can be used. The proposed method is helpful to estimate hydrokinetic potential for gauged sites for preliminary purpose avoiding need for measurements and site visits which in turn cut the cost for these works in addition to the time thus helping efficient planning.

References

- [1] Deependra Singh, Devender Singh, K. S. Verma, "Multiobjective Optimization for DG Planning With Load Models", IEEE Transactions on Power Systems, Year: 2009, Volume: 24, Issue: 1, pp: 427 - 436.
- [2] Herman Jacobus Vermaak, Kanzumba Kusakana, Sandile Philip Koko, "Status of Micro-hydrokinetic River Technology in Rural Applications: A Review of Literature", Renewable and Sustainable Energy Reviews, Volume 29, January 2014, pp. 625-633.
- [3] Hydrokinetic resource assessment and mapping, http://www.eere.energy.gov/water/pdfs/riverine_hydrokinetic_resource_assessment_and_mapping.pdf
- [4] The Betz limit - and the Maximum Efficiency for Horizontal Axis Wind Turbines, <http://www.wind-power-program.com/betz.htm>, Accessed on 2016-09-19 and 2017-19-02.
- [5] Paul Duvoy, Horacio Toniolo, " HYDROKAL: A Module for in-Stream Hydrokinetic Resource Assessment", Computers & Geosciences, Volume 39, February 2012, pp. 171-181.
- [6] A. Tarpanelli, L. Brocca, S. Barbetta, M. Faruolo, T. Lacava, T. Moramarco, "Coupling MODIS and Radar Altimetry Data for Discharge Estimation in Poorly Gauged River Basins", IEEE Journal of Selected Topics in Applied Earth Observations and Remote Sensing, Year: 2015, Volume: 8, Issue: 1, pp. 141-148.
- [7] A. Mutule; A. Kalnacs, "Hydro-energy Potential Estimation for Hydrokinetic Power Plants", Electric Power Engineering (EPE), Proceedings of the 2014 15th International Scientific Conference on Year: 2014, pp. 297 - 300, DOI: 10.1109/EPE.2014.6839540, IEEE Conference Publications.
- [8] Hydrologic Engineering Center, <http://www.hec.usace.army.mil/software/hecras/>, Accessed on 2016-09-01 and 2017-19-02
- [9] Maria Kartezhnikova, Thomas M. Ravens, "Hydraulic impacts of hydrokinetic devices", Renewable Energy, Volume 66, June 2014, pp 425-432 Wave Energy,